

Accepted Manuscript

An Experimental/Numerical investigation into the main driving force for crack propagation in uni-directional fibre-reinforced composite laminae

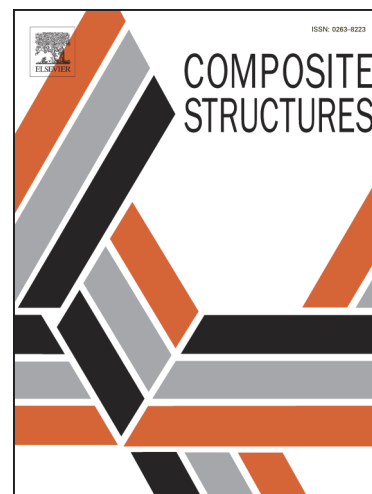
L.M.A. Cahill, S. Natarajan, S.P.A. Bordas, R.M. O'Higgins, C.T. McCarthy

PII: S0263-8223(13)00258-4

DOI: <http://dx.doi.org/10.1016/j.compstruct.2013.05.039>

Reference: COST 5183

To appear in: *Composite Structures*



Please cite this article as: Cahill, L.M.A., Natarajan, S., Bordas, S.P.A., O'Higgins, R.M., McCarthy, C.T., An Experimental/Numerical investigation into the main driving force for crack propagation in uni-directional fibre-reinforced composite laminae, *Composite Structures* (2013), doi: <http://dx.doi.org/10.1016/j.compstruct.2013.05.039>

This is a PDF file of an unedited manuscript that has been accepted for publication. As a service to our customers we are providing this early version of the manuscript. The manuscript will undergo copyediting, typesetting, and review of the resulting proof before it is published in its final form. Please note that during the production process errors may be discovered which could affect the content, and all legal disclaimers that apply to the journal pertain.

An Experimental/Numerical investigation into the main driving force for crack propagation in uni-directional fibre-reinforced composite laminae

L. M. A. Cahill, S. Natarajan^a, S. P. A. Bordas^{b,1}, R. M. O'Higgins, C. T. McCarthy*

Irish Centre for Composites Research (IComp), Materials and Surface Science Institute (MSSI), University of Limerick, Ireland

^a*School of Civil and Environmental Engineering, The University of New South Wales, Sydney, Australia*

^b*Cardiff School of Engineering, Theoretical, applied and computational mechanics, Cardiff University, Queen's Buildings, The Parade, Cardiff CF24 3AA, Wales, UK*

Abstract

This paper presents an enriched finite element method to simulate the growth of cracks in linear elastic, aerospace composite materials. The model and its discretisation are also validated through a complete experimental test series. Stress intensity factors are calculated by means of an interaction integral. To enable this, we propose application of (1) a modified approach to the standard interaction integral for heterogeneous orthotropic materials where material interfaces are present; (2) a modified maximum hoop stress criterion is proposed for obtaining the crack propagation direction at each step, and we show that the “standard” maximum hoop stress criterion which had been frequently used to date in literature, is unable to reproduce experimental results. The influence of crack description, material orientation along with the presence of holes and multi-material structures are investigated. It is found, for aerospace composite materials with $\frac{E_1}{E_2}$ ratios of approximately 10, that the material orientation is the driving factor in crack propagation. This is found even for specimens with a material orientation of 90° , which were previously found to cause difficulty in both damage mechanics and discrete crack models e.g. by the extended finite element method (XFEM). The results also show the crack will predominantly propagate along the fibre direction, regardless of the specimen geometry, loading conditions or presence of voids.

Keywords: 1, Composites; 2, Fracture Mechanics; 3, Crack Growth; 4, Extended Finite Element Method; 5, Material Interfaces;

1. Introduction

Composite materials are already widely used in engineering structures, especially in the aeronautical, and, indeed, the aerospace industries where their high specific strength and stiffness make them ideally suited to reduce weight. However, a major weakness of these laminated materials is that they are prone to delamination at both the interface, between the plies (interlaminar) and within plies (intralaminar). This hinders reliable prediction of their durability in service. It is therefore of primary importance to devise reliable experimental and numerical techniques to study and predict the behaviour of existing materials, as well as engineer new damage tolerant composites capable of sustaining the increasingly demanding conditions in which they are used. Composites are, by definition, made up of several phases which, together, provide the resulting material with the combined strengths of its individual components. Advanced composites are composed of stiff elastic fibres bonded together by a toughened epoxy matrix, to form a lamina; numerous lamina are then bonded together to form a laminate. At the first level of simplification, each layer (i.e. lamina) can be considered as a linear, elastic, orthotropic material. In order to predict the intralaminar failure in such a lamina, it is important to be able to accurately simulate crack performance and propagation under loading. Techniques extensively used to predict the behaviour and growth of cracks include continuum damage mechanics [1], [2] or progressive damage analysis [3], [4], [5]. In these approaches, the crack or cracks are not modelled explicitly, but their effect is accounted for by locally modifying the elastic moduli of material points that have been determined to be damaged. While these approaches are relatively computationally efficient and accurate, they suffer from a number of drawbacks, such as mesh sensitivity and an inability to capture ply splitting, which is a major contributor to the size effect experienced in open-hole composites testing [6]. To alleviate these difficulties, discrete crack approaches such as those relying on the partition of unity methods (PUM) [7] can be used instead. In the PU framework, arbitrary functions are added to the standard polynomial finite element (FE) space in order to improve the approximation power of the resulting numerical method. In particular, the extended finite element method (XFEM)

*Correspondence to Email : conor.mccarthy@ul.ie, Tel: +35361234334, Fax: +35361202944

¹Email : stephane.bordas@alum.northwestern.edu

[8], which belongs to the class of partition of unity methods, allows simulation of crack propagation without remeshing by introducing two classes of enrichment functions: discontinuous enrichment to capture the displacement jump through the crack faces and near-tip asymptotic enrichment to capture the stress singularity at the crack tip in linear elastic fracture mechanics (LEFM). Although a vast body of literature has examined cracking in various types of composite materials using different techniques, for example, Rebière *et al.*, [9] employed a combined analytical and a three-dimensional finite element study to study transverse and longitudinal cracks in laminates, Ramanujam *et al.*, [10] studied fatigue crack growth using a combined experimental and computational investigation and meshfree method and cracking particle methods were employed in [11, 12, 13, 14, 15] to study arbitrary evolving cracks in reinforced concrete structures. Yet, to date, there is only a limited amount of work in the literature which involves XFEM for crack propagation simulation in orthotropic materials. This is despite the fact that such a method, which has been shown to perform efficiently for damage tolerance assessment of complex structures [16], [17], [18] and also holds promise for the analysis of the durability of composite materials by virtue of its ability to describe arbitrary crack growth without remeshing and with relatively coarse meshes. The most significant contributions in the area of orthotropic materials have come from [19], [20], [21] who developed new crack tip enrichment functions to effectively capture the crack tip displacement fields within linear elastic orthotropic materials. Further developments in dynamics allowed the study of propagation in orthotropic materials using XFEM [22]. Other topical work has focussed on interlaminar delamination [23] and cracks in functionally graded composites [24], [25].

In this paper, a new tool based on the extended finite element method (XFEM) which allows to simulate the growth of arbitrary cracks in orthotropic materials is devised, analysed and validated experimentally. The technique builds on recent work of Asadpoure and Mohammadi [19], which concentrates on the calculation of stress intensity factors (SIFs) and extends it to allow the accurate simulation of crack growth through an orthotropic material. The model is thoroughly validated by a bespoke test series and further applied to more complex problems to study the driving factors for crack propagation in orthotropic laminae.

This work relies on the key postulate that an orthotropic material definition is suitable for simulation of a uni-directional composite lamina and validates this postulate experimentally. The present paper employs a modified maximum hoop stress criterion to calculate the direction of crack propagation as well as a new domain integral method for heterogeneous materials. The proposed model is capable of dealing with multi-material structures under complex loading conditions. The outline of the paper is as follows; Section 2 briefly outlines the stress and displacement theory for an orthotropic body. In Section 3, the extended finite element method is presented for modelling of strong and weak discontinuities in orthotropic materials. Section 4 poses the fracture criteria of the model, while Section 5 introduces the experimental test series. Section 6 - Section 9 present validation and further numerical examples using the model developed. The major conclusions are drawn in Section 10.

2. Stresses and displacements at the crack tip of an orthotropic body

Assume an anisotropic body with a crack subjected to arbitrary forces with general boundary conditions. According to Lekhnitskii [26] by using the equilibrium and compatibility conditions, a fourth-order partial differential ‘characteristic’ equation can be obtained;

$$a_{11}\mu^4 - 2a_{16}\mu^3 + (2a_{12} + a_{66})\mu^2 - 2a_{26} + \mu a_{22} = 0 \quad (1)$$

where a_{11} , a_{22} , a_{16} , a_{12} , a_{26} , $a_{66} \in \mathbb{R}$ and are the elastic compliances. The roots of Equation 1 are always complex or purely imaginary ($\mu_k = \mu_{kx} + i\mu_{ky}$, $k = 1, 2$) and occur in conjugate pairs as $\mu_1, \bar{\mu}_1$ and $\mu_2, \bar{\mu}_2$ [26]. From these, Sih *et al.* [27] derived the two-dimensional displacement and stress fields in the vicinity of the crack-tip using analytical functions and complex variables. These stress components and displacements are later employed in this work for calculation of SIFs using an interaction integral. Full details of these fields may be found in [27], or indeed more recently in [19].

3. Enriched finite element approximations for linear elastic orthotropic fracture mechanics

The principle of the extended finite element method is to locally enrich the standard FEM basis through a local partition of unity, enabling the exact reproduction of these enrichment functions by the enriched approximation. These enrichment functions are chosen so as to best replicate known features about the exact problem. In particular, for crack problems treated by the extended finite element method (XFEM), the displacement field is augmented by a discontinuous function, allowing to describe the displacement jump across the crack faces without requiring the mesh to conform to those, and asymptotic enrichment functions enabling the approximation to reproduce, with coarse meshes, the large gradients near the crack tips.

3.1. Enrichment functions

The enriched approximation is thus designed to take account of any discontinuities, known behaviour or any *a-priori* knowledge about the solution sought. It was recently demonstrated by Menk and Bordas [28], [29] that numerically determined

enrichment functions can be used to simulate arbitrary cracks and wedges in composite or anisotropic materials.² For crack modelling, two classes of analytical enrichment functions are used. The Heaviside, step function or split enrichment function,

$$H(x) = \begin{cases} -1 & x \leq 0 \\ +1 & x > 0 \end{cases} \quad (2)$$

confers the approximation the power to reproduce any discontinuous function, and thus the jump in displacement through the crack faces. In order to model the crack tip singularity, the nodes about the crack tip(s) are enriched with crack tip or branch functions, first proposed in [8]. These branch functions span the first order terms of the Williams' expansion [34] of the asymptotic displacement field around a crack tip in a linear elastic material. For orthotropic materials, attempts have been made to derive the crack tip enrichment functions by [19] (See also Menk and Bordas [28] where those are computed numerically). The asymptotic fields for orthotropic materials are given in [19] as,

$$\{F_a\}_{1 \leq a \leq 4}(r, \theta) = \sqrt{r} \left\{ \cos \frac{\theta_1}{2} \sqrt{g_1(\theta)}, \cos \frac{\theta_2}{2} \sqrt{g_2(\theta)}, \sin \frac{\theta_1}{2} \sqrt{g_1(\theta)}, \sin \frac{\theta_2}{2} \sqrt{g_2(\theta)} \right\} \quad (3)$$

where θ_1 , θ_2 , $g_1(\theta)$ and $g_2(\theta)$ are functions of θ , the angle about the crack tip, and are given as,

$$g_k(\theta) = \sqrt{(\cos \theta + \mu_{kx} \sin \theta)^2 + (\mu_{ky} \sin \theta)^2} \quad (4)$$

$$\theta_k = \arctan \left(\frac{\mu_{ky} \sin \theta}{\cos \theta + \mu_{kx} \sin \theta} \right) \quad (5)$$

and $\mu_k = \mu_{kx} + i\mu_{ky}$ are the roots of the characteristic equation, (Equation 1). These functions are used as orthotropic enrichment for the remainder of this work.

For material interface modelling, an enrichment function with a kink (i.e. a discontinuous first derivative) is necessary to represent arbitrary material interfaces independently of the mesh. The absolute value function

$$A(x) = \left| \sum_I \phi_I(x) N_I(x) \right| \quad (6)$$

(where ϕ_I is the level set function) remains continuous in the displacement space but confers a jump in the strain field (weak discontinuity) across the material interfaces. For further details see [35], [36], [37], implementation aspects are provided in [38].

4. Fracture criteria and stress intensity factor evaluation

The problem at hand is the quasi-static propagation of cracks in an orthotropic linear elastic material. To simulate linear elastic fracture, it is assumed that a pre-crack is present in the material.³ The stress intensity factor or 'K' fracture criterion is chosen due to recent advances in experimental validation of the calculation of stress intensity factors by digital image correlation, as in [40], as well as its relative ease of implementation.

4.1. The interaction integral for SIF evaluation

In orthotropic materials cracks are generally subjected to mixed mode loading. Hence, two SIFs are required, one for each mode (mode 1 and mode 2). In order to evaluate these, the interaction integral of [41] is utilised. The interaction integral is an extension to the widely accepted J -Integral of Rice [42]. This path independent integral which may be interpreted as the energy flowing through a contour encompassing the crack tip, per unit crack advance is defined in [42] as,

$$J = \int_{\Gamma} \left(W \delta_{1j} - \sigma_{ij} \frac{\partial u_j}{\partial x_1} \right) n_j d\Gamma \quad (7)$$

where Γ is an arbitrary contour surrounding the crack-tip which encloses no other cracks or discontinuities, weak or strong. W is the strain energy density for a linear-elastic material, n_j is the j th component of the outward unit normal to Γ , δ is the Kronecker delta second order tensor and the co-ordinates are taken to be the local crack-tip co-ordinates with the x-axis parallel to the crack

²This idea is similar to spider XFEM [30] and parametric enrichment [31]. Ultimately, a posteriori error estimators could be used to help derive the enrichment functions ([32] and [33]).

³Note that the variational theory of fracture proposed by Francfort and Marigo [39] allows a prediction of both the nucleation and propagation of linear elastic cracks within a single framework and thereby provides a generalisation of Griffith's theory of fracture.

face. For the sake of implementation simplicity and accuracy using XFEM, the contour integral is transformed into an equivalent domain integral (EDI), which is written as,

$$J = \int_A (\sigma_{ij} u_{i,1} - W \delta_{1j}) q_{,j} dA \quad (8)$$

where A is an area surrounding the crack-tip and would be the interior region of Γ and q is a function smoothly varying from $q=1$ at the crack-tip to $q=0$ at the exterior boundary, Γ . Therefore, the derivative is constant. By relating the energy release rates G_i ($i=1,2$) to J , J can be shown to be related to the SIFs of a crack in a homogeneous anisotropic plate by,

$$J = c_{11} K_I^2 + c_{12} K_I K_{II} + c_{22} K_{II}^2 \quad (9)$$

where

$$c_{11} = -\frac{a_{22}}{2} \mathfrak{J} \left[\frac{\mu_1 + \mu_2}{\mu_1 \mu_2} \right] \quad (10)$$

$$c_{22} = -\frac{a_{11}}{2} \mathfrak{J} (\mu_1 + \mu_2) \quad (11)$$

$$c_{12} = -\frac{a_{22}}{2} \mathfrak{J} \left[\frac{1}{\mu_1 \mu_2} \right] + \frac{a_{11}}{2} \mathfrak{J} (\mu_1 \mu_2) \quad (12)$$

However, this is not sufficient for evaluating the SIFs independently in the case of a mixed mode problem. Therefore, in accordance with Wang [41], if Equation 9 is used in conjunction with the conservation law for two independent equilibrium states of the linearly elastic solid, both SIFs can be computed. By defining two equilibrium states, and in accordance with the Principle of Superposition, the J -integral for the superimposed (combined) state is shown to be,

$$J^S = J + J^{aux} + M \quad (13)$$

where, in domain form,

$$M = \int_A (\sigma_{ij} u_{i,1}^{aux} + \sigma_{ij}^{aux} u_{i,1} - W^{(1,2)} \delta_{1j}) q_{,j} dA \quad (14)$$

and W , the strain energy density is defined as,

$$W^{(1,2)} = \frac{1}{2} (\sigma_{ij} \varepsilon_{ij}^{aux} + \sigma_{ij}^{aux} \varepsilon_{ij}) \quad (15)$$

where superscript ‘aux’ stands for the auxiliary state. Stresses and strains for the auxiliary state should be chosen as to satisfy both the equilibrium equation and traction-free boundary condition on the crack surface in the area A . The choice of the displacement and stress fields in the vicinity of the crack-tip for this work is provided by Sih [27]. After some manipulation, the following equation is obtained to evaluate M ,

$$M = 2c_{11} K_I + K_I^{aux} + c_{12} (K_I K_{II}^{aux} + K_I^{aux} K_{II}) + c_{22} K_{II} + K_{II}^{aux} \quad (16)$$

By calculating M from both Equation 14 and Equation 16 and solving a system of linear algebraic equations the actual mixed mode SIFs are obtained,

$$M^1 = 2c_{11} K_I + c_{12} K_{II} \quad (17)$$

$$M^2 = c_{12} K_I + 2c_{22} K_{II} \quad (18)$$

In the case of multi-material models or models involving material interfaces, should the J -domain cross the material interface, the path independence will be lost and the resulting values invalid. The interested reader is referred to the review paper on stress intensity factor calculations within an XFE framework [43]. An important adaptation to the interaction integral was introduced in [44] for non-homogeneous, isotropic materials with arbitrarily continuous properties. This approach takes account of the difference in material properties between the crack tip and the Gauss points contained within the J -domain. The modified M integral is now given by:

$$M = \int_A (\sigma_{ij} u_{i,1}^{aux} + \sigma_{ij}^{aux} u_{i,1} - W^{(1,2)} \delta_{1j}) q_{,j} dA + \int_A (\sigma_{ij} [S_{ijkl}^{tip} - S_{ijkl}] \sigma_{kl,1}^{aux} q dA) \quad (19)$$

where, S_{ijkl}^{tip} and S_{ijkl} refer to the compliance tensor at the crack tip, and The additional terms will disappear naturally where no material interfaces exist.

4.2. Crack propagation direction criterion

In order to accurately predict crack growth in an orthotropic material a meaningful crack propagation direction at each increment is required.⁴ The crack propagation direction for this work will be calculated based on the maximum circumferential stress criterion. The criterion was originally developed by [45] for isotropic materials and extended to orthotropic materials by [46] and is commonly used in XFE analysis due to its efficiency and ease of implementation. The basis of the criterion is that the crack will propagate in the direction where the hoop or circumferential stress (σ_θ) is maximum. However, when the criterion is applied to orthotropic materials, it must be reformulated to account for angular variation of fracture toughness in the material. Saouma [46] proposed that the spatial variation of the fracture toughness may be given by,

$$K_{IC}^\theta = K_{IC}^1 \cos^2 \theta + K_{IC}^2 \sin^2 \theta \quad (20)$$

where K_{IC}^1 and K_{IC}^2 refer to the fracture toughness of the material along the 1- and 2- directions respectively. However, this required two separate fracture toughness test on the material to obtain K_{IC}^1 and K_{IC}^2 . Saouma suggested that a remedy to this requirement may be to consider the ratio of the fracture toughness in both directions as equal to the ratio of the elastic moduli. As such, the material stiffness ratio may be used in place of the fracture toughness values as:

$$\frac{E_2}{E_1} = \frac{K_{IC}^1}{K_{IC}^2} \quad (21)$$

Hence it is suggested that the maximum hoop stress should be normalised by the angular variation of fracture toughness giving the criterion as:

$$\frac{\sigma_\theta}{\frac{E_2}{E_1} \cos^2 \theta + \sin^2 \theta} \quad (22)$$

where the numerator refers to the hoop stress at a point about the crack tip.

In this work, the denominator is shifted to account for the relative angle of the crack to the material orientation at all times throughout propagation. This allows an accurate incremental analysis. The new criterion then becomes:

$$\frac{\sigma_\theta}{\frac{E_2}{E_1} \cos^2((\theta - \theta_{material} + \alpha) + \sin^2(\theta - \theta_{material} + \alpha))} \quad (23)$$

where α is the crack angle and $\theta_{material}$ the material orientation. This criterion will be used in all numerical experiments carried out for the remainder of this paper.

5. Experimental Study

The material used in this work is unidirectional carbon-fiber reinforced epoxy HTA/6376 manufactured by Hexcel. The elastic properties, measured in a previous investigation [3], are shown in Table 1. E_1 is the longitudinal Young's modulus, E_2 the transverse Young's modulus, G_{12} refers to the shear modulus and ν_{12} is the major Poisson's ratio. The pre-impregnated plies were laid up into an 8-ply (1 mm thick) unidirectional configuration for a range of material orientations: 0°, 30°, 45°, 60°, and 90° and cured according to Hexel's specifications. The specimens, one single edge notched (SEN) specimen and one centre notch tension (CNT) specimen were machined to their final geometry, shown in Figure 1, with the narrow cracks applied by a tungsten carbide end mill.

The specimens were tested using a Zwick/Roell 100kN universal straining frame equipped with hydraulic grips. A controlled loading rate (machine crosshead displacement rate) of 0.1mm/sec and a 100kN load cell were used for all tests carried out. The specimens were gripped with 50mm × 50mm grips designed for composite materials. Each test was recorded using a Photron SA1.1 ultra high speed camera system with 1024 × 1024 pixel resolution, capturing upwards of 125 frames per second (fps) and up to a maximum of 100,000 fps.

6. Static Verification

The model developed is used to generate load-displacement data for the composite specimens tested experimentally, up to the point of failure. The model predicts accurately the load-displacement behaviour for all material orientations. For material orientations from 0° - 60° the crosshead displacement compares well to the predicted displacement of the model as shown in Figure 2 (a) for a sample 45° specimen. The results for the 90° orientations require an extensometer to accurately capture the displacement (which was due to the stiffness of the material in the loading direction). The displacement over the gauge length (50mm) of the extensometer was captured well by the model as shown in Figure 2 (b). Whilst confirming the model, these results also highlight that no other damage mechanisms occur prior to matrix cracking.

⁴For the purpose of this work the growth is assumed *quasi-static* crack growth, where inertia forces are neglected and the body is assumed in equilibrium at all times.

7. Benchmark SIF problems

The stress intensity factor predicted by the XFEM are compared to previously published results. Three sample specimens, with geometries detailed in Figure 3 and material properties given in Table 1 are examined assuming plane stress conditions. The first problem of an edge crack (SEN) in an orthotropic material is deemed to converge with a mesh of 2,576 dofs (based on a fully uniform square mesh). The SIF (where Norm $K_i = \frac{K_i}{\sqrt{\pi a}}$) results for varying θ (material orientation) are shown in Figures 4 (a) and (b) and are in good correlation with those of Asadpoure and Mohammadi [19]. The second benchmark problem, shown in Figure 3 (b) is that of a centre crack (CNT) with variable crack orientation (α) and fixed material orientation. Again good agreement is found to the reference result of [19] (Figures 4 (c) and (d)). The final specimen examined is a finite sized edge crack specimen, loaded in shear (Figure 3 (c)). The K_I and K_{II} values for a large range of material orientations ($\theta = -90^\circ$ to 90°) are shown to reflect well the results of [47] as detailed in Figures 4 (e) and (f) respectively.

8. Crack Propagation

It is observed experimentally that the SEN specimens, due to their geometry tend to bear lower loads before failure compared to the CNT specimens. In this section the model is used to numerically predict the direction in which the crack will propagate upon failure and the results compared to our experimental data. Using the criterion detailed in Section 4.2, the direction of propagation is calculated at each increment and the crack advanced a fixed amount in that direction for thirteen increments. A further study concluded that, in the present examples, the increment size, which is the only arbitrary parameter in this study, had no significant impact on the crack trajectory.

The experimental results of the SEN specimen are also shown in Figure 5 (a)(ii)-(e)(ii), the crack is shown to always propagate in the fibre direction (1-direction). This was shown to occur irrespectively of the initial fibre angle. A high speed video camera, with a frame recording rate of 250 frames per second, was used to film the growth of the crack, and it was found that the crack propagated in less than $\frac{1}{250}$ of a second, quick enough to be considered instantaneous. The experimental results for propagation angle compare very well with the current XFE predictions (Table 2), but contrast with previous XFE predictions (on a similar carbon fibre epoxy material) of [22]⁵ and other dual boundary element analysis predictions of [48] which were based on the standard maximum hoop stress criterion which, we show in this paper is inadequate for the materials considered here. Initial propagation angles are presented due to the instantaneous nature of the crack propagation uncovered experimentally. The numerical predictions for the orthotropic specimen with a predefined edge crack (SEN), for the same range of material orientations are shown in Figures 5 (a)(i)-(e)(i). The initial pre-crack is highlighted by the thick grey line and the propagation pattern is shown thereafter. The crack is predicted by the current model to grow in a direction very close to that of the fibre- or 1-direction in agreement with the experimental findings.

The propagation direction of the experimental CNT specimens reflects that of the SEN specimens and remained along the stiffer fibre direction at all times (Figure 6 (a)(ii)-(e)(ii)). The numerical predictions of the XFEM, for the same range of material orientations are shown in Figures 6 (a)(i)-(e)(i). Again, the crack is found to grow in the direction of the fibre (or 1-direction) with initial propagation angles identical to the SEN specimen (shown as experimental in Table 2).

8.1. Crack splitting at 90°

In studying the experimental propagation results it is observed that splitting of the crack in two directions occurs at a material angle of 90° (Figure 5 (e)(ii)). On more detailed investigation, what is found when individual frames of the high speed recording are examined, is that the crack initially splits either upwards or downwards (at 90° to the original crack), with a -90° propagation direction found to be equally as likely as $+90^\circ$ propagation direction (Figure 8). The current XFEM results are also shown to predict two similar valued peaks (as maximum peaks of the normalised circumferential stress) for the propagation direction, as can be seen in Figure 7 (a). The model hence predicts well the phenomena observed experimentally. In this work, this is found only to occur for the 90° specimen and does not occur numerically even at a material angle of 80° , as shown in Figure 7 (b).

9. Further Numerical Examples

Having rigorously verified the load-displacement behaviour, SIF predictions and crack propagation criterion, the XFE model developed is applied to a variety of more complex composite crack problems in 2D plane stress.

⁵These are approximate initial propagation angles, see [22]

9.1. Crack Geometry: effect on propagation

Section 7 examined the effect on K_I and K_{II} of the crack orientation with respect to the loading direction. In order to investigate the impact of the initial crack angle on the crack trajectory, propagation for a non-zero initial crack angle is considered. The crack trajectory is numerically predicted to be along the fibre direction at all times, as shown for the 45° crack with fibre angle of 30° and 60° off-axis in Figure 9 (a) and (b) respectively. It may be concluded that, in the absence of inclusions, other cracks or voids, the crack trajectory in a similar aerospace unidirectional composite material will at all times remain exclusively along the fibre direction. These findings highlight the significance of the material orientation in determining the angle of crack propagation. In this type of aerospace composite, where the E_1 stiffness is far greater than the E_2 stiffness the propagation path is controlled by the fibre direction regardless of the crack geometry.

9.2. Bonded Orthotropic Plates: effect on SIFs

The XFE model is applied to bonded strips of carbon epoxy HTA/6376 assuming a plane stress condition. All strips are composed of HTA/6376, however, the material orientations (θ_i) are allowed to vary from strip to strip. Various locations of interfaces (h_i) are also examined Figure (Figure 10). A crack is located centrally in the first material, the second material remains crack free. A uniform load is applied. The effect of varying material orientation of the second strip (θ_2) is initially examined. Figure 11 (a) illustrates the impact of varying the material orientation of the non-cracked side from 0° - 90° whilst the material containing the crack remains at a fixed orientation of 0° (for $2a=4$). A square specimen is examined of side length 40. K_I is normalised as $\frac{K_I}{P\sqrt{a}}$. Model 1 refers to results when $2h_1 = 2h_2 = 20$. The study ascertained that the K_I value is inversely related to θ_2 . The maximum value of K_I is found when both strips are at 0° . The observed decrease is found despite the location of the material interface, as is shown in Figure 11 (a) for model 2 when $2h_1 = 30$, and for model 3 when $2h_1 = 10$. The severity of the decrease in K_I is controlled by the size of the second material strip. A narrow strip, as found in model 2 causes much more gradual decrease. A wider second strip has a much larger impact on the K_I of material 1.

It should be noted that the decrease in K_I when the second material varies from 0° - 90° is based upon perfectly bonded structures. K_I refers solely to the stress intensity factor at the crack tip. While material 2 at 90° would see the stiffer fibres bear the load, and hence reduce the stress induced on the crack tip in material 1, the difference in the stiffness of the two strips may have a significant effect on the interface of the two strips. This difference in deformation caused would most likely create large stresses at the interface of these two materials in a practical structure. However, this is beyond the scope of this work.

Examining this effect for a range of material 1 (cracked material) orientations indicates a general decrease in K_I as the second material moves from 0° - 90° . In this work the interface is located $2h_1 = 20$. The decrease is significantly more pronounced for lower material 1 orientations (0° - 45°) as shown in Figure 11 (b). As the cracked material becomes more fibre dominated with respect to the loading direction the influence of the second materials orientation reduces. An unusual pattern is observed when the material 1 orientation is 90° , as the material orientation of material two increases the K_I value is also found to increase slightly. This may indicate that the 90° ply benefits from co-existing with a lower material orientation ply (strip) such as a 45° . This may be attributed to the fact the deformation of material 2 is much greater than that of material 1 at lower θ_2 material orientations, due to the lower stiffness. This high deformation may close in upon or shield the cracked side.

9.3. Plates containing open holes: effect on propagation

The presence of holes in plates has been shown to disturb the stress and strain fields and influence the propagation of cracks within these plates. An interesting complex example for PMMA was examined by [49] which found that the crack trajectory for an isotropic material was heavily dependant upon the initial crack geometry relative to the holes within the plate. The problems examined by [49] are here examined for a unidirectional composite material with properties of HTA/6376. The model and crack geometries are shown in Figure 12 and details of dimensions for the 2 examples studied are given in Table 3.

In order to investigate the initial impact of the addition of three holes to a composite plate, the SIF for each example was compared to the sample when no holes were present. The addition of the holes, which are reasonably remote from the initial crack was found to have very little impact on the initial K_I and K_{II} values.

The propagation behaviour for the two crack locations Example 1 and Example 2 (Table 3) are then examined. The crack location and geometry in the PMMA samples Bittencourt *et al* [49] examined were found to have a significant impact on the crack trajectory. However, the results from the orthotropic model are found to be less dramatic due to the dominance (detailed earlier) of the fibre orientation in dictating the crack trajectory. As shown in Figure 13 for example 1 the crack propagation remains along the fibre direction at all times and is not influenced by the presence of holes in the specimen. The results for example 2 are very similar with the crack choosing to propagate along the fibre direction at all times.

10. Conclusions

This paper presented and rigorously validated a complete orthotropic material model for failure of fibre-reinforced composite laminae. The model was discretised by an extended-finite element method enabling the capture of propagating cracks independently of background mesh. It was shown that the standard maximum hoop stress criterion, used throughout numerical fracture mechanics is unsuitable to study fracture in orthotropic materials and another, modified criterion, was applied. The influence of crack geometry, material orientation and multiple materials were investigated. It was found that, for all cases examined, the crack trajectory follows the fibre- or 1-direction. Of particular interest is the model's capability to capture the splitting (along the fibre direction) in the 90° off-axis specimen. Such capability, not seen in continuum damage approaches, may be very useful to capture the hole size effect, observed in the testing of open-hole composites [6], where matrix splitting is a key damage mechanism. The modified maximum hoop stress criterion was shown to perform much better than the standard maximum hoop stress criterion used in [22] and [48]. The predicted crack paths correlate almost exactly with experimental findings. These experiments also revealed that the crack propagation occurred instantaneously ($< \frac{1}{250}$ of a second). Bonded orthotropic (uni-directional composite) strips were also examined and it was found that varying the non-cracked material orientation from 0° - 90° results in a gradual decrease in the mode I stress intensity factor K_I of the cracked specimen. As the cracked strips orientation is varied, it is found that in fact a 90° cracked strip may in fact benefit from pairing with a lower material orientation. Such a model could be very useful to optimise lay-ups in composite laminates. A composite structure containing holes was also examined. It was found that in contrast to isotropic materials, in a thin uni-directional composite material, the crack trajectory is unaffected by proximity to open holes (voids). The crack grows along the fibre direction at all times regardless of the presence of open holes.

11. Acknowledgements

The authors wish to acknowledge the funding provided by the Irish Research Council for Science, Engineering and Technology (IRCSET). Stéphane Bordas also thanks partial funding for his time provided by 1) the EPSRC under grant EP/G042705/1 Increased Reliability for Industrially Relevant Automatic Crack Growth Simulation with the eXtended Finite Element Method. 2) the European Research Council Starting Independent Research Grant (ERC Stg grant agreement No. 279578) entitled Towards real time multiscale simulation of cutting in non-linear materials with applications to surgical simulation and computer guided surgery. S Natarajan would like to acknowledge the financial support of the School of Civil and Environmental Engineering, The University of New South Wales for his research fellowship since Sep 2012.

References

- [1] P. Ladevéze and E. LeDantec. Damage modelling of the elementary ply for laminated composites. *Composites Science and Technology*, 43:257–267, 1992.
- [2] Roberto C. Pavan, Guillermo J. Creus, and Samir Maghous. A simplified approach to continuous damage of composite materials and micromechanical analysis. *Composite Structures*, 91(1):84 – 94, 2009.
- [3] C.T. McCarthy, R.M. O'Higgins, and R.M. Frizzell. A cubic spline implementation of non-linear shear behaviour in three-dimensional progressive damage models for composite laminates. *Composite Structures*, 92(1):173 – 181, 2010.
- [4] H.K. Lee and D.K. Shin. A computational investigation of crack evolution and interactions of microcracks and particles in particle-reinforced brittle composites. *Composite Structures*, 64(3-4):419 – 431, 2004.
- [5] P. Kerfriden, J. C. Passieux, and S. P. A. Bordas. Local/global model order reduction strategy for the simulation of quasi-brittle fracture. *International Journal for Numerical Methods in Engineering*, 89(2):154–179, 2012.
- [6] R.M. O'Higgins, M.A. McCarthy, and C.T. McCarthy. Comparison of open hole tension characteristics of high strength glass and carbon fibre-reinforced composite materials. *Composites Science and Technology*, 68:2770–2778, 2008.
- [7] I Babuška and JM Melenk. The partition of unity finite element method. *International Journal for Numerical Methods in Engineering*, 40:727–758, 1997.
- [8] T. Belytschko and T. Black. Elastic crack growth in finite elements with minimal remeshing. *International Journal for Numerical Methods in Engineering*, 45:601–620, 1999.
- [9] J.-L. Rebire, M.-N. Matallah, and D. Gamby. Initiation and growth of transverse and longitudinal cracks in composite cross-ply laminates. *Composite Structures*, 53(2):173 – 187, 2001.
- [10] Narayanan Ramanujam, Pavankiran Vaddadi, Toshio Nakamura, and Raman P. Singh. Interlaminar fatigue crack growth of cross-ply composites under thermal cycles. *Composite Structures*, 85(2):175 – 187, 2008.
- [11] T. Rabczuk and T. Belytschko. Application of particle methods to static fracture of reinforced concrete structures. *International Journal of Fracture*, 137(1-4):19–49, 2006.
- [12] T. Rabczuk and T. Belytschko. Cracking particles: a simplified meshfree method for arbitrary evolving cracks. *International Journal for Numerical Methods in Engineering*, 61(13):2316–2343, 2004.
- [13] T. Rabczuk and T. Belytschko. A three-dimensional large deformation meshfree method for arbitrary evolving cracks. *Computer Methods in Applied Mechanics and Engineering*, 196(2930):2777 – 2799, 2007.
- [14] Timon Rabczuk, Goangseup Zi, Stéphane Bordas, and Hung Nguyen-Xuan. A geometrically non-linear three-dimensional cohesive crack method for reinforced concrete structures. *Engineering Fracture Mechanics*, 75(16):4740 – 4758, 2008.
- [15] Timon Rabczuk, Goangseup Zi, Stéphane Bordas, and Hung Nguyen-Xuan. A simple and robust three-dimensional cracking-particle method without enrichment. *Computer Methods in Applied Mechanics and Engineering*, 199(3740):2437 – 2455, 2010.
- [16] Stéphane Bordas and Brian Moran. Enriched finite elements and level sets for damage tolerance assessment of complex structures. *Engineering Fracture Mechanics*, 73(9):1176 – 1201, 2006.

- [17] E. Wyart, D. Coulon, M. Duflo, T. Pardoen, J.-F. Remacle, and F. Lani. A substructured fe-shell/xfem-3d method for crack analysis in thin-walled structures. *International Journal for Numerical Methods in Engineering*, 72(7):757–779, 2007.
- [18] L. Cahill, C. McCarthy, and S. Bordas. The extended finite element method: A review. In *Proceedings of the 6th International Conference on Engineering Computational Technology*, Athens, 2008.
- [19] A. Asadpoure and S. Mohammadi. Developing new enrichment functions for crack simulation in orthotropic media by the extended finite element method. *International Journal for Numerical Methods in Engineering*, 69:2150–2172, 2007.
- [20] A. Asadpoure, S. Mohammadi, and A. Vafai. Modeling crack in orthotropic media using a coupled finite element and partition of unity methods. *Finite Elements in Analysis and Design*, 42(13):1165–1175, 2006.
- [21] Alireza Asadpoure, Soheil Mohammadi, and Abolhasan Vafai. Crack analysis in orthotropic media using the extended finite element method. *Thin-Walled Structures*, 44(9):1031 – 1038, 2006.
- [22] D. Motamedi and S. Mohammadi. Dynamic crack propagation analysis of orthotropic media by the extended finite element method. *International Journal of Fracture*, 161:21–39, 2010.
- [23] S. Esna Ashari and S. Mohammadi. Delamination analysis of composites by new orthotropic bimaterial extended finite element method. *International Journal for Numerical Methods in Engineering*, 86(13):1507–1543, 2011.
- [24] Hamid Bayesteh and Soheil Mohammadi. Xfem fracture analysis of orthotropic functionally graded materials. *Composites Part B: Engineering*, 44(1):8 – 25, 2013.
- [25] S. Natarajan, P.M. Baiz, S. Bordas, T. Rabczuk, and P. Kerfriden. Natural frequencies of cracked functionally graded material plates by the extended finite element method. *Composite Structures*, 93(11):3082 – 3092, 2011.
- [26] SG Lekhnitskii. *Theory of an Anisotropic Elastic Body*. Holden-Day: San Francisco, 1963.
- [27] G. C. Sih, P. C. Paris, and G. R. Irwin. On cracks in rectilinearly anisotropic bodies. *International Journal of Fracture Mechanics*, 1(3):189–203, 1965.
- [28] A. Menk and S.P.A. Bordas. Numerically determined enrichment functions for the extended finite element method and applications to bi-material anisotropic fracture and polycrystals. *International Journal for Numerical Methods in Engineering*, 23, 2009.
- [29] Alexander Menk and Stéphane P. A. Bordas. A robust preconditioning technique for the extended finite element method. *International Journal for Numerical Methods in Engineering*, 85(13):1609–1632, 2011.
- [30] P. Laborde, E. Chahine and Y. Renard. Spider-xfem, an extended finite element variant for partially unknown crack-tip displacement. *European Journal of Computational Mechanics*, 15(5-7):625–636, 2008.
- [31] Haim Waisman and Ted Belytschko. Parametric enrichment adaptivity by the extended finite element method. *Int J Numer Meth Eng*, 73(12):1671–1692, Jan 2008.
- [32] Stéphane Pierre Alain Bordas, Marc Duflo, and Phong Le. A simple error estimator for extended finite elements. *Communications in Numerical Methods in Engineering*, 24(11):961–971, 2008.
- [33] Stéphane Pierre Alain Bordas and Marc Duflo. Derivative recovery and a posteriori error estimate for extended finite elements. *Computer Methods in Applied Mechanics and Engineering*, 196(35-36):3381–3399, Jan 2007.
- [34] M L Williams. On the stress distribution at the base of a stationary crack. *Journal of Applied Mechanics*, 24:109–114, 1957.
- [35] N. Moes, M. Cloirec, P. Cartraud, and J. F. Remacle. A computational approach to handle complex microstructure geometries. *Computer Methods in Applied Mechanics and Engineering*, 192(28-30):3163 – 3177, 2003.
- [36] Timon Rabczuk, Stéphane Bordas, and Goangseup Zi. On three-dimensional modelling of crack growth using partition of unity methods. *Computers & Structures*, 88:1391 – 1411, 2010.
- [37] Mohammed Moumnassi, Salim Belouettar, ric Bchet, Stéphane P.A. Bordas, Didier Quoirin, and Michel Potier-Ferry. Finite element analysis on implicitly defined domains: An accurate representation based on arbitrary parametric surfaces. *Computer Methods in Applied Mechanics and Engineering*, 200(58):774 – 796, 2011.
- [38] Stéphane Pierre Alain Bordas, Phu Vinh Nguyen, Cyrille Dunant, Amor Guidoum, and Hung Nguyen-Dang. An extended finite element library. *Int J Numer Meth Eng*, 71(6):703–732, Jan 2007.
- [39] G. A. Francfort and J. J. Marigo. Revisiting brittle fracture as an energy minimization problem. *Journal of the Mechanics and Physics of Solids*, 46(8):1319 – 1342, 1998.
- [40] Mogadpalli G. P. and Parameswaran V. Determination of stress intensity factor for cracks in orthotropic composite materials using digital image correlation. *Strain*, 44(6):446–452, 2008.
- [41] S. S. Wang, J. F. Yau, and H. T. Corten. A mixed-mode crack analysis of rectilinear anisotropic solids using conservation laws of elasticity. *International Journal of Fracture*, 16(3):247–259, 1980.
- [42] J.R. Rice. A path independent integral and approximate analysis of strain concentration by notches and cracks. *Journal of Applied Mechanics*, 35:379–, 1968.
- [43] Marc Duflo. A study of the representation of cracks with level sets. *International Journal for Numerical Methods in Engineering*, 70(11):1261–1302, 2007.
- [44] Hongjun Yu, Linzhi Wu, Licheng Guo, Shanyi Du, and Qilin He. Investigation of mixed-mode stress intensity factors for nonhomogeneous materials using an interaction integral method. *International Journal of Solids and Structures*, 46(20):3710 – 3724, 2009.
- [45] F. Erdogan and G.C. Sih. On the crack extension in plates under plane loading and transverse shear. *Journal of Basic Engineering*, pages 519–527, 1963.
- [46] VE Saouma, ML Ayari, and DA Leavell. Mixed mode crack propagation in homogenous anisotropic solids. *Engineering Fracture Mechanics*, 27(2s):171–189, 1987.
- [47] R. K. L. Su and H. Y. Sun. Numerical solutions of two-dimensional anisotropic crack problems. *International Journal of Solids and Structures*, 40(18):4615 – 4635, 2003.
- [48] M. H. Aliabadi and P. Sollero. Crack growth analysis in homogeneous orthotropic laminates. *Composites Science and Technology*, 58(10):1697 – 1703, 1998.
- [49] T. N. Bittencourt, P. A. Wawrzynek, A. R. Ingraffea, and J. L. Sousa. Quasi-automatic simulation of crack propagation for 2d LEFM problems. *Engineering Fracture Mechanics*, 55(2):321 – 334, 1996.

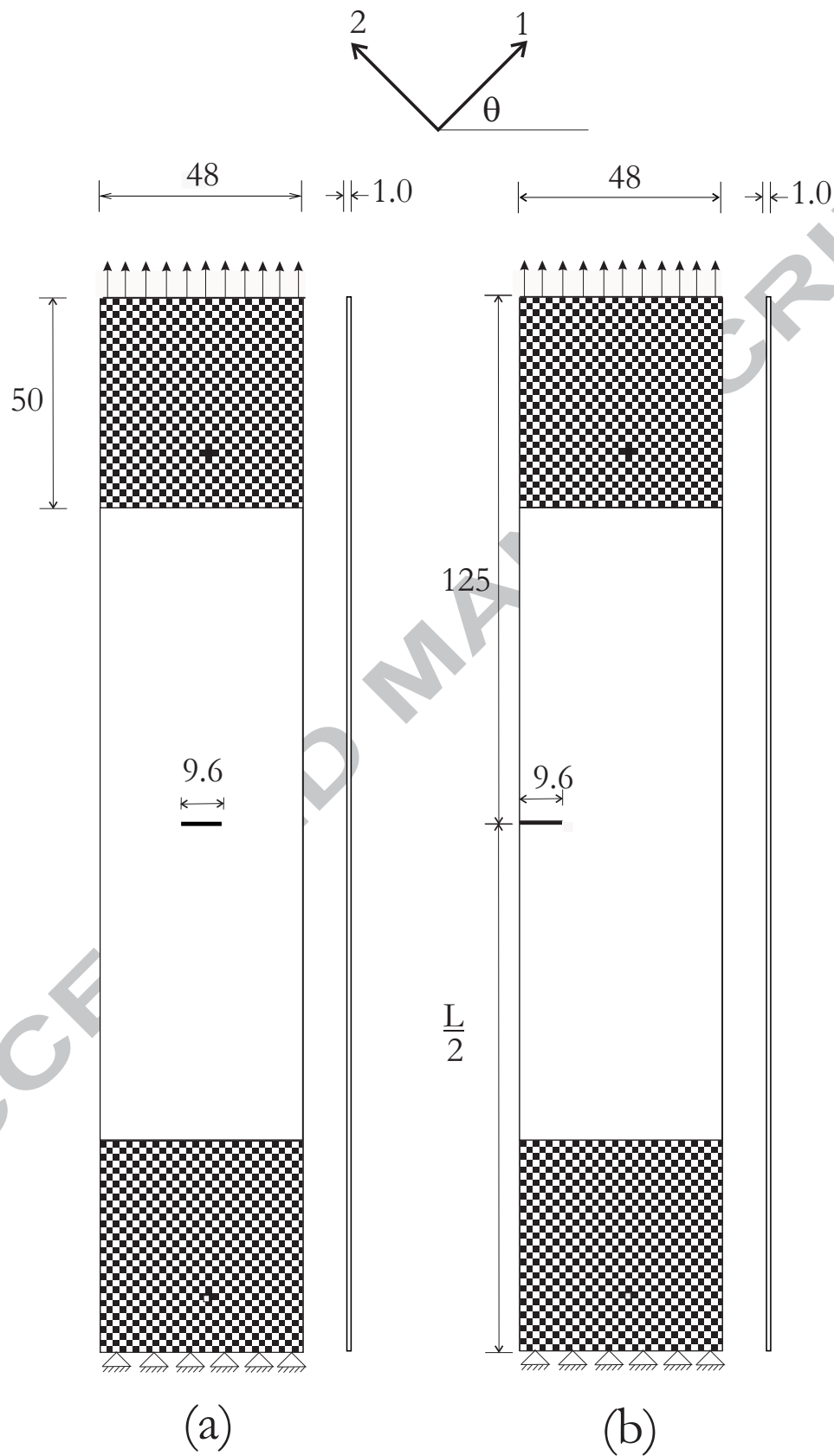


Figure 1: Geometry of (a) single edge notch specimen (b) centre notch tension specimen where all dimensions are in mm

Table 1: Model Properties

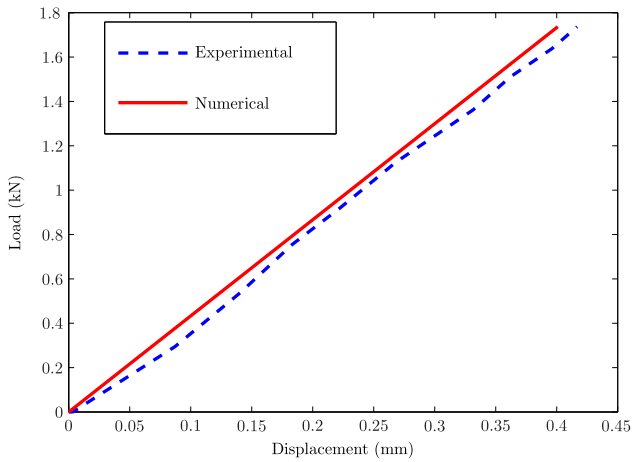
Model	E_1 (GPa)	E_2 (GPa)	G_{12} (GPa)	ν_{21}
Experimental	139	10	5.2	0.3
Edge (Tension and Shear)	114.8	11.7	9.66	0.21
Centre	3.5	12	3	0.7

Table 2: Initial Propagation Angles

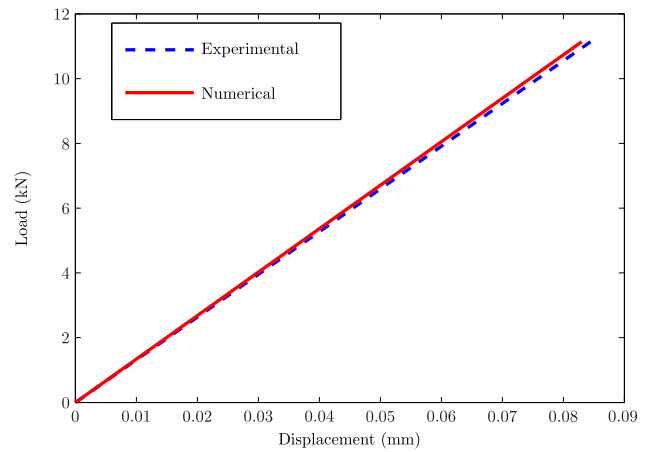
Fibre Orientation	0	30	45	60	90
θ_{inc} Experimental	0	30	45	60	90
θ_{inc} Current XFEM	0	29	43	57	83
θ_{inc} Dynamic XFEM [22]	0	-55	-31	-38	0
θ_{inc} Dual Boundary Element [48]	-17	-26	-36	-49	0

Table 3: Three Hole Structure Model Dimensions

Example	a	b	P
1	5	1.5	1
2	6	1	1



(a)



(b)

Figure 2: Sample Experimental and Numerical load - displacement behaviour of (a) 45 degree off-axis CNT specimen and (b) 90 degree off axis CNT specimen up to the point of fracture

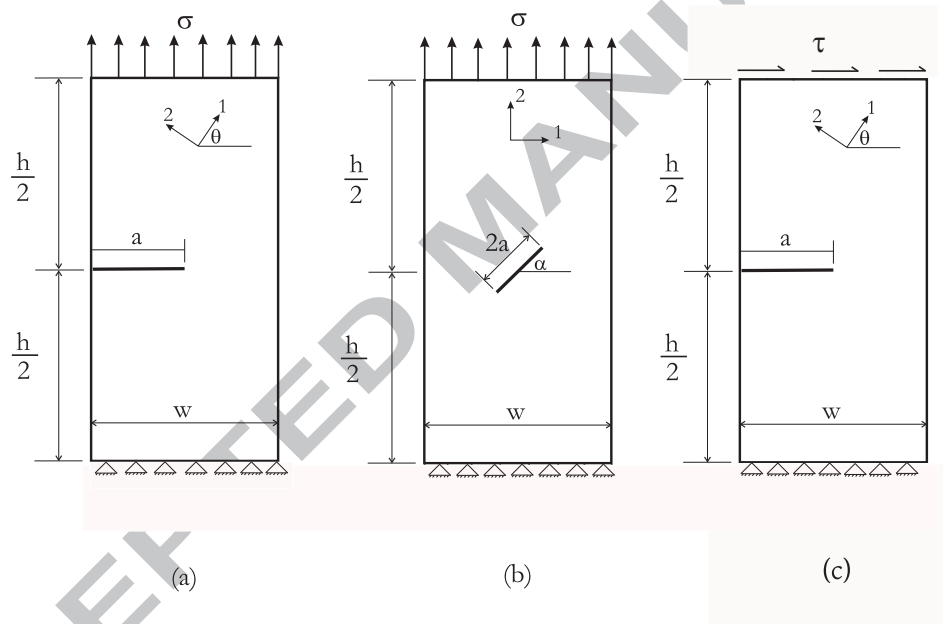


Figure 3: Problem descriptions for (a) edge crack (b) centre crack and (c) edge crack in shear

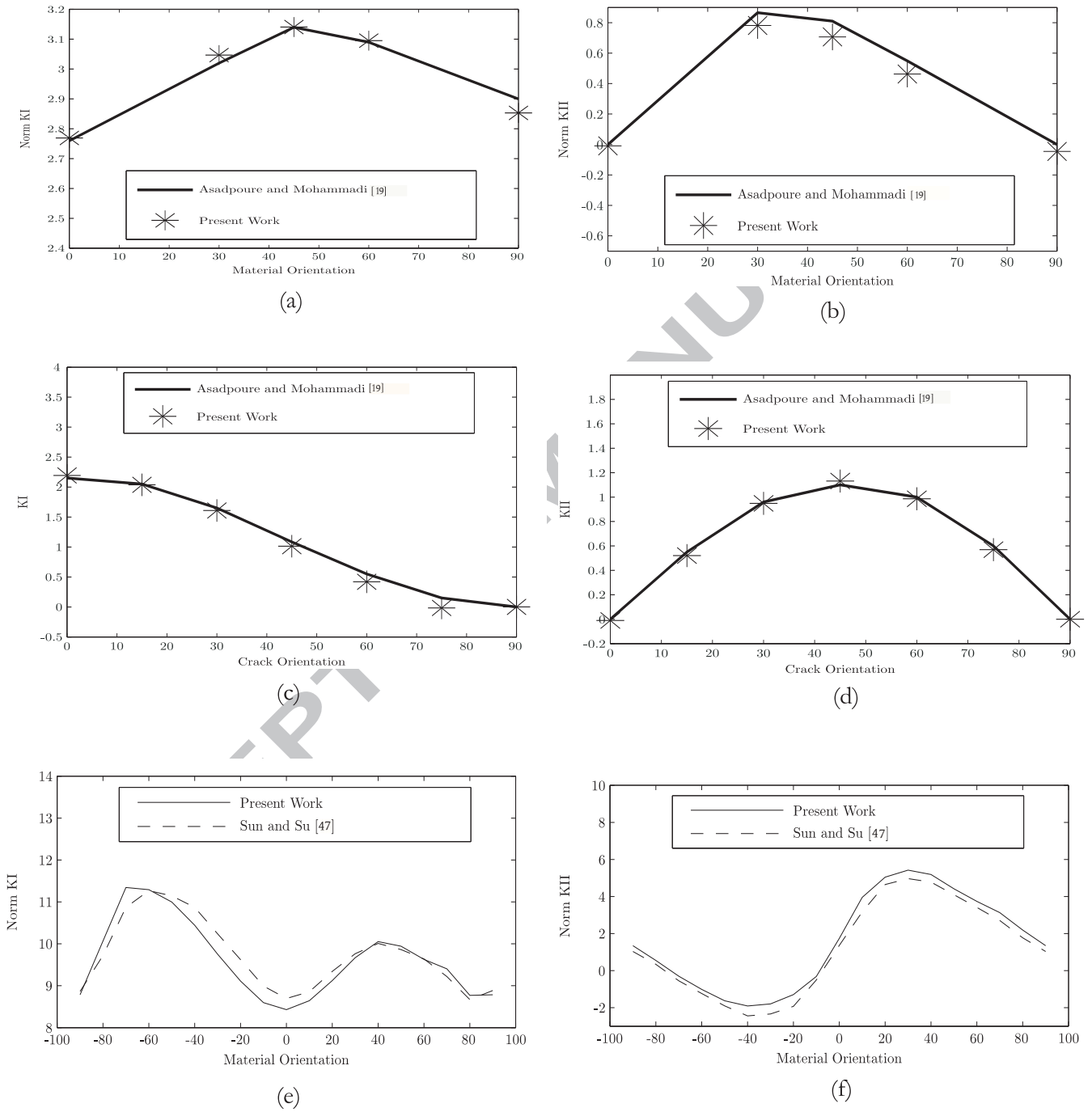


Figure 4: Benchmark Results for (a) and (b) the edge cracked specimen, (c) and (d) the centre crack specimen and (e) and (f) the edge crack in shear specimen

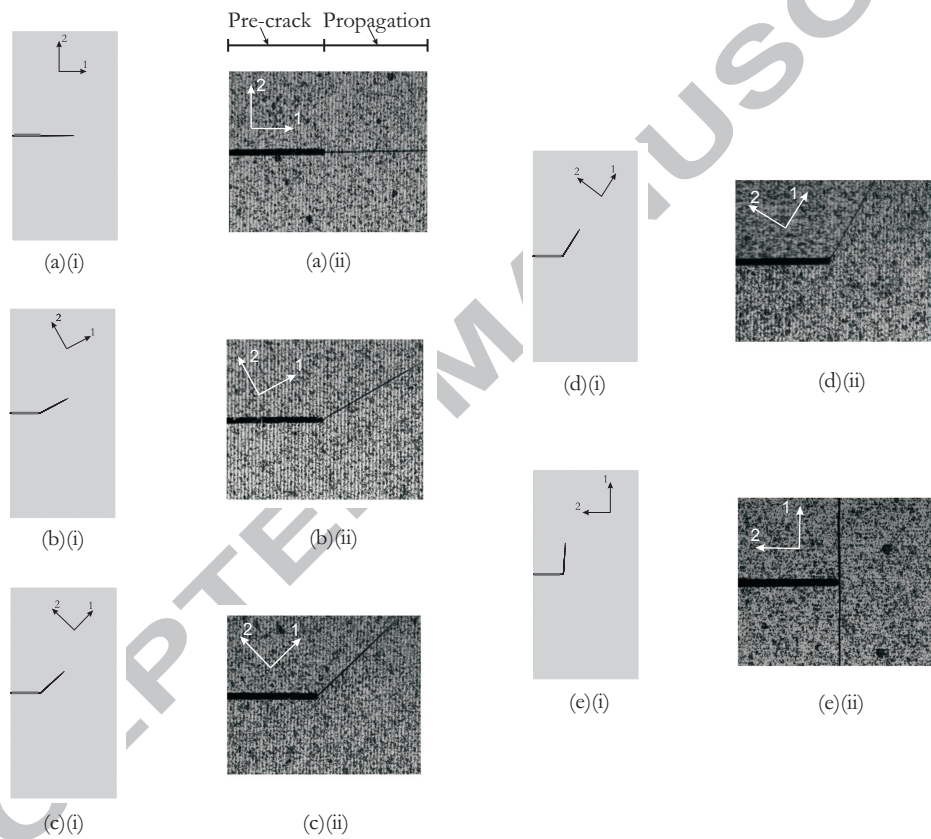


Figure 5: Numerical (i) and Experimental (ii) Propagation results for (a) 0, (b) 30, (c) 45, (d) 60 and (e) 90 degree off-axis SEN specimens of Carbon Fibre HTA-6376

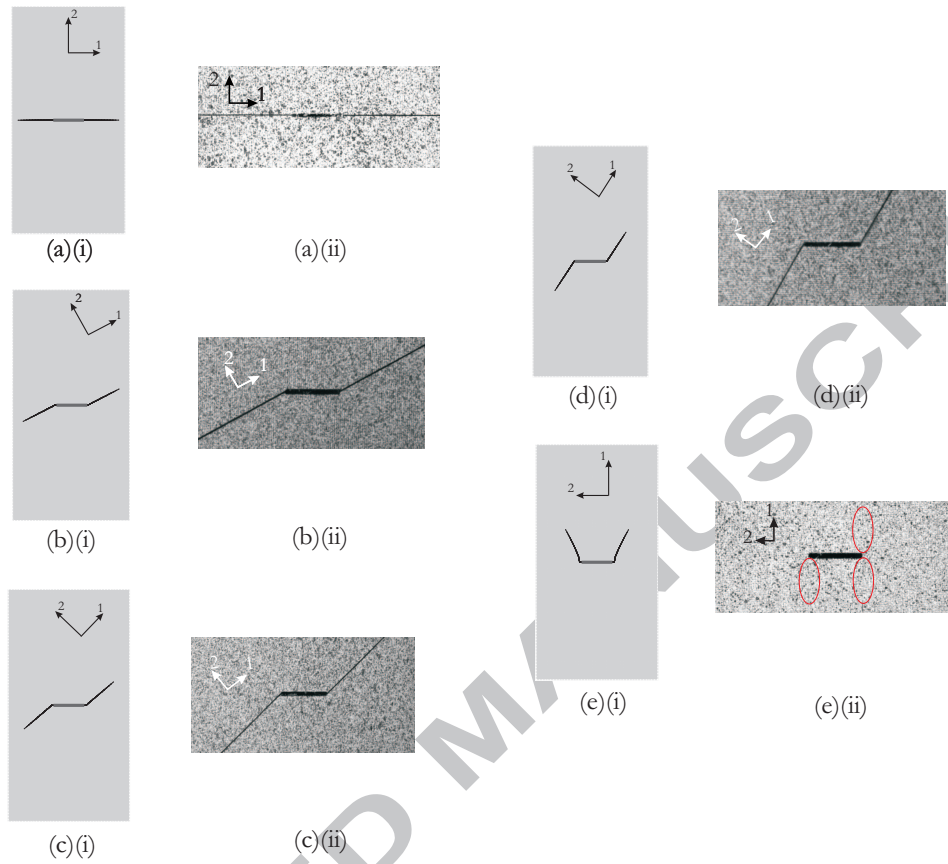


Figure 6: Numerical (i) and Experimental (ii) Propagation results for (a) 0, (b) 30, (c) 45, (d) 60 and (e) 90 degree off-axis CNT specimens of Carbon Fibre HTA-6376

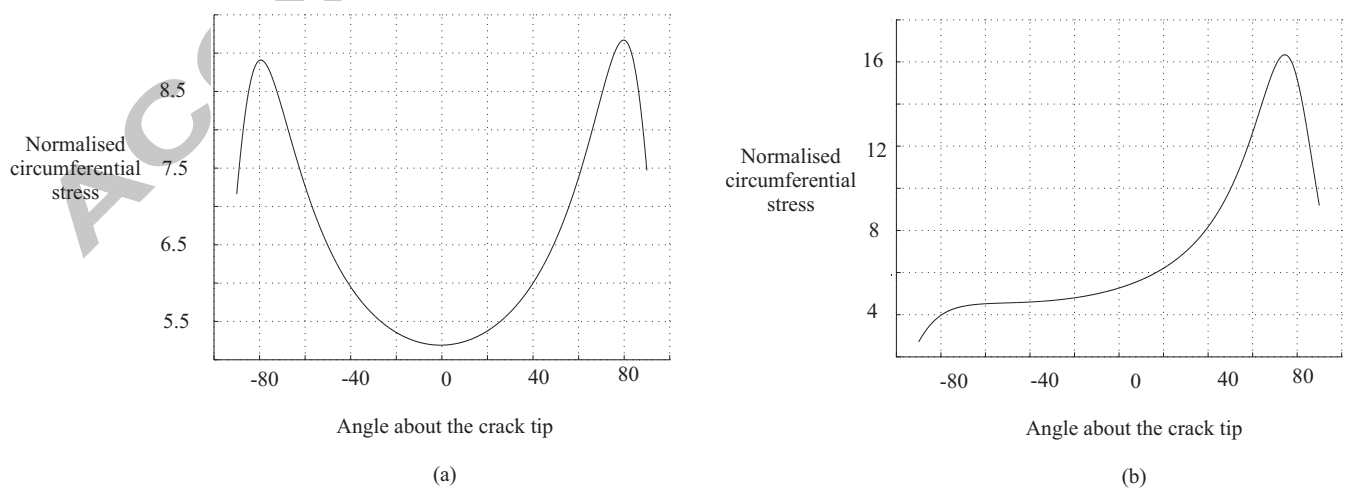
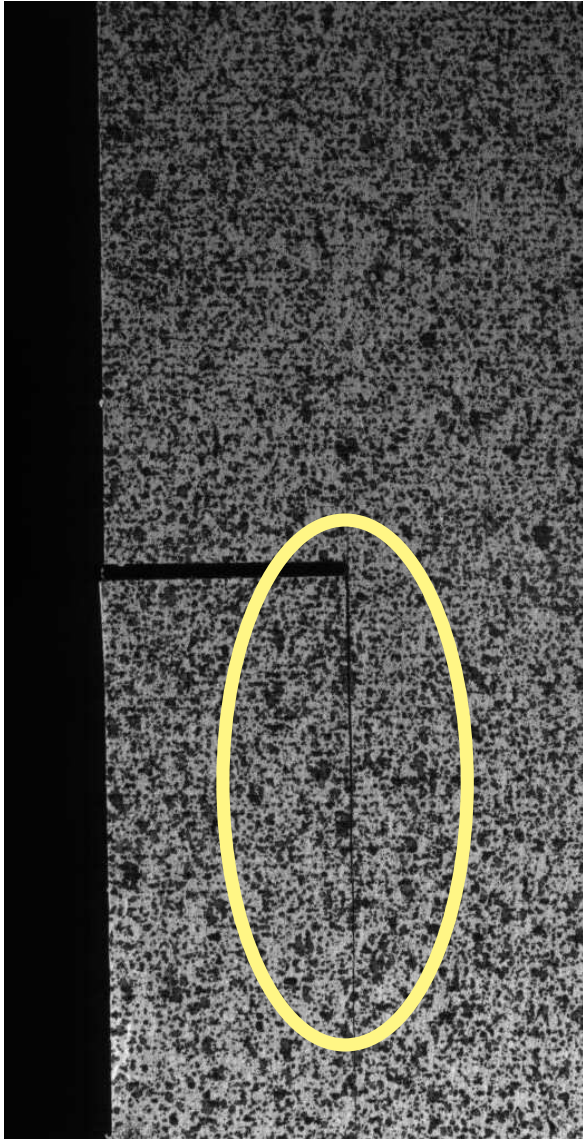


Figure 7: Variation of normalised hoop stress about crack tip for (a) 90 and (b) 80 degree off-axis specimen



(a)



(b)

Figure 8: Propagation results for 2 Single Edge Notched specimens for 90° off axis, the crack trajectory for each highlighted

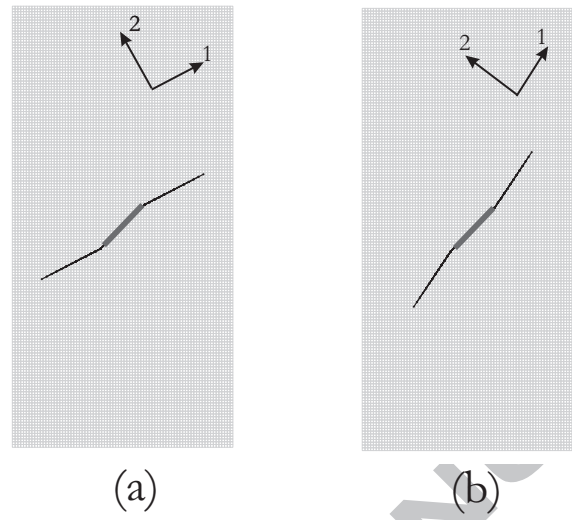


Figure 9: Angled 45° centre cracks for (a) 30 and (b) 60 degree off-axis specimen

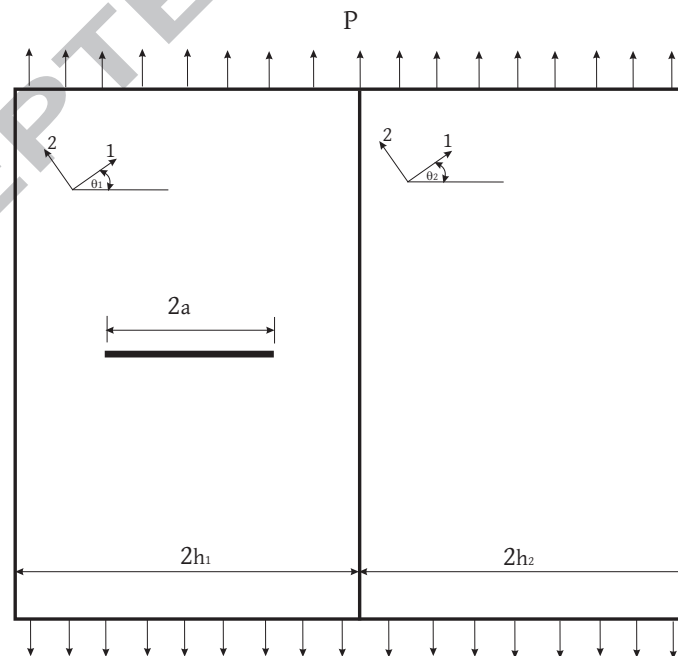


Figure 10: Bonded Orthotropic Structure of HTA/6376 where θ_1 refers to the material orientation in the left hand side and θ_2 in the right hand side

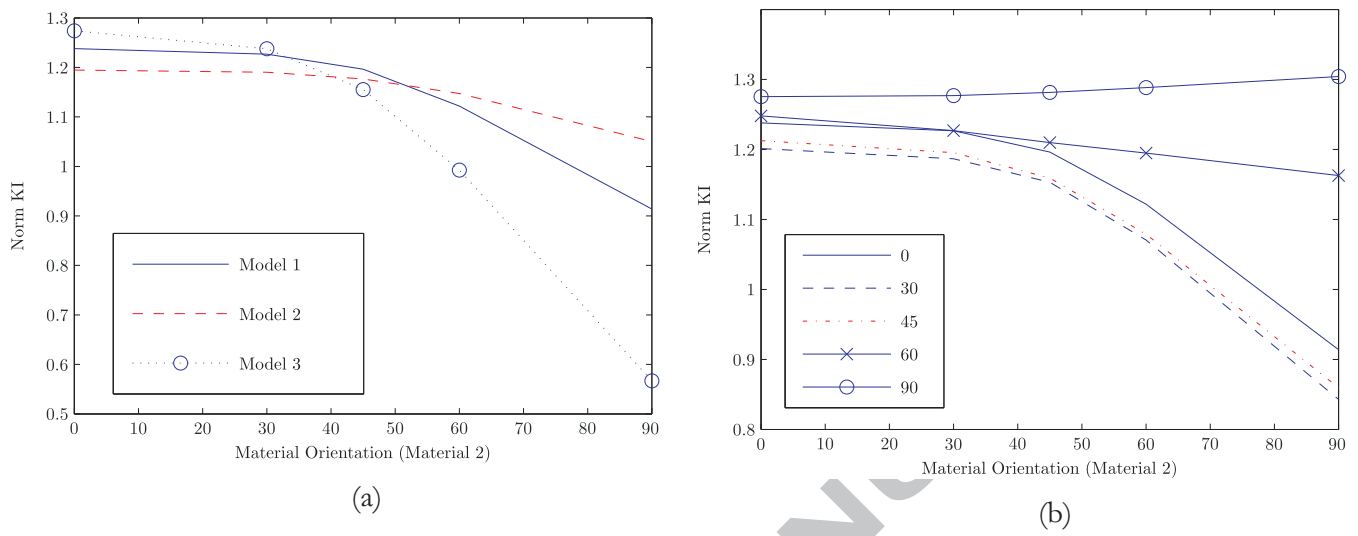


Figure 11: Change in KI with variable θ_2 for (a) $\theta_1 = 0$, and (b) variable θ_1

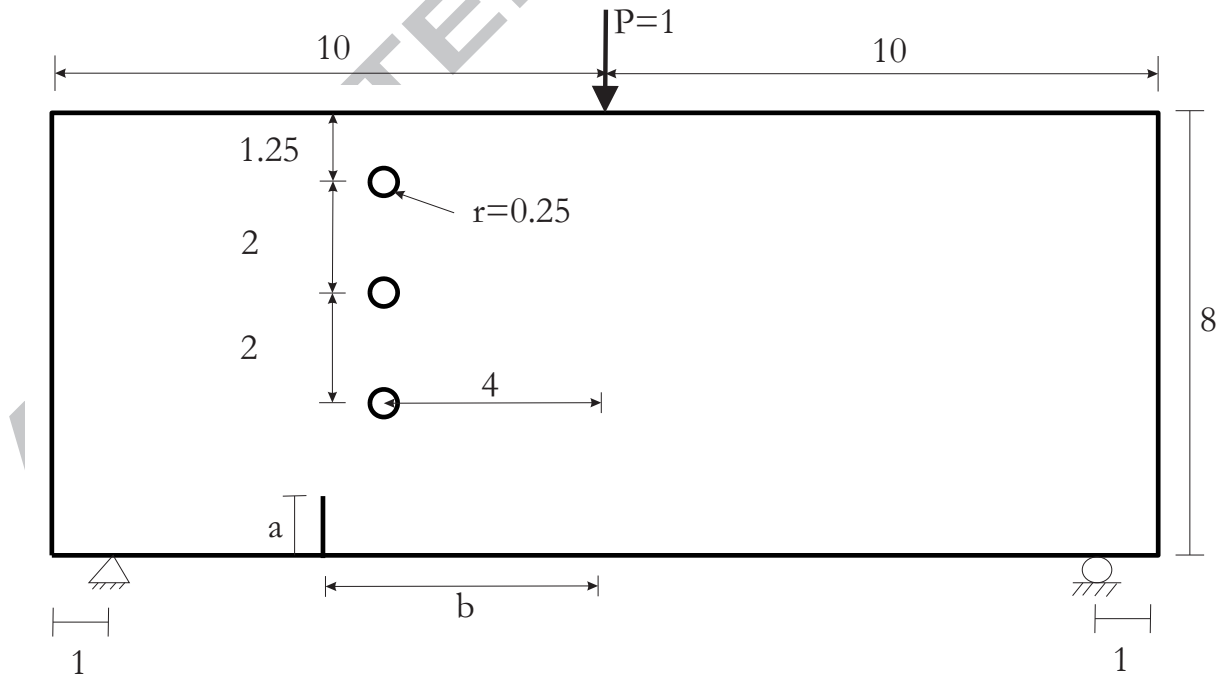


Figure 12: Composite structure with three holes present in close proximity to an edge crack

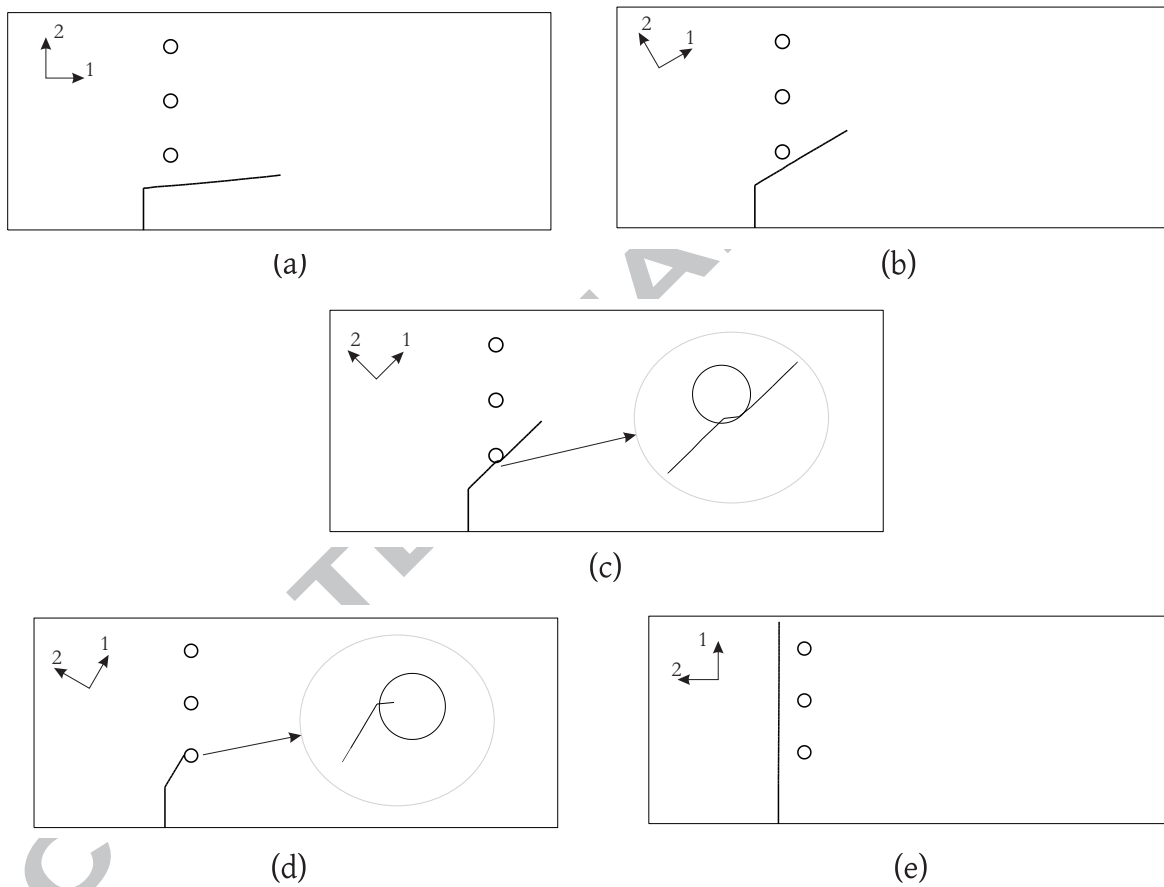


Figure 13: Propagation results for Example 1 for (a) 0, (b) 30, (c) 45, (d) 60 and (e) 90 degree off-axis specimens